J Solid State Electrochem (2006) 10: 651–658
DOI 10.1007/s10008-006-0128-9

ORIGINAL PAPER

D. I. Bronin · B. L. Kuzin · I. Yu. Yaroslavtsev · N. M. Bogdanovich

Behavior of manganite electrodes in contact with LSGM electrolyte: the nature of low electrochemical activity

Received: 27 December 2005 / Accepted: 12 January 2006 / Published online: 21 March 2006

Abstract The electrochemical cells with electrodes based on $La_{0.8}Sr_{0.2}MnO_3$ (LSM) and supporting solid electrolytes $La_{0.88}Sr_{0.12}Ga_{0.82}Mg_{0.18}O_{2.85}$ (LSGM) and $Ce_{0.80}Sm_{0.20}O_{1.90}$ (SDC) were studied comparatively. Characteristics of LSM electrodes and composite electrodes comprising a mixture of LSM and electrolytes of different origins [LSGM, SDC, and $Zr_{0.82}Sc_{0.18}O_{1.91}$ (SSZ) in the mass ratio of 1:1] were analyzed. It was shown that: 1) the electrode polarization conductivity and the ohmic resistance of the cells with the LSM–LSGM composite electrodes on the LSGM and SDC electrolytes had very similar values, while they were largely different from all the other electrodes, 2) the electrochemical activity of the electrodes on the SDC electrolyte was much higher than on the LSGM electrolyte, and 3) the ohmic resistance of the cells with the SDC electrolyte corresponded to the electrolyte resistance, whereas, the ohmic resistance of the cells with the LSGM electrolyte was much larger than the electrolyte resistance. The obtained results are due to the interaction between the LSM and LSM-containing electrodes with the LSGM electrolyte during sintering, leading to the formation of a product with a very low conductivity.

Keywords Lanthanum gallate · Ceria · Lanthanum manganite · Cathode

Introduction

The direct conversion of the chemical energy of a fuel to the electric power in fuel cells is one of the most promising ways of improving the ecological situation in megapolises and is an efficient use of natural fuels for power supply for various transport facilities and for electricity consumers located far from electric power stations. In addition to high efficiency, attractive features of fuel cells include the absence of moving parts, easy maintenance, and noiseless running.

One of the most actively developing directions in the field of fuel cells is concerned with solid-oxide fuel cells, which allow the use of diverse fuels. Thanks to wide-scale comprehensive studies initiated in 1960s, operating temperatures of solid-oxide fuel cells were reduced from the traditional high-temperature range (900–1,000° C) to an intermediate-temperature range (500–800° C). The decrease in the operating temperature was due, in particular, to the discovery of new high-conduction electrolytes based on $LaGaO_3$ [1, 2] and reappraisal of the negative attitude to CeO_2-based solid electrolytes (see, for example, [3]). The practicability of fuel cells with these electrolytes was demonstrated, for example, in [4–7].

A significant factor that limits the efficiency of fuel cells at intermediate temperatures is that the decrease in the operating temperature leads to a high polarization of the electrodes and, hence, a large power loss. Therefore, a topical problem facing the researchers is the development of electrodes that provide a high electrochemical activity and a stable long-term operation at 500–800° C. The solution to this problem requires, on one hand, a profound understanding of the origin of electrode polarization and, on the other hand, the knowledge of such materials science issues as the interaction between the contacting materials of the electrode and the electrolyte, a stable morphology of the electrodes, and similar thermal expansion coefficients of the solid electrolyte and the electrodes.

At present, oxide cathodes based on $La(Sr)MnO_3$ (LSM) have received the most attention from the viewpoint of materials science and of their electrochemical behavior. This material satisfies most requirements imposed on fuel-cell electrodes. Specifically, it has a sufficiently high electric conductivity, namely, up to 300 S/cm at 700° C, depending on the strontium concentration [8], while the thermal expansion coefficient of LSM (11.6×10^{-6} K^{-1} at temperatures below 800° C for $La_{0.8}Sr_{0.2}MnO_3$ [9]) allows

D. I. Bronin (✉) · B. L. Kuzin · I. Y. Yaroslavtsev · N. M. Bogdanovich
Institute of High Temperature Electrochemistry,
S. Kovalevskoy 22,
620219 Ekaterinburg, Russia
e-mail: bronin@ihte.uran.ru

its use with electrolytes based on ZrO_2, CeO_2, and $LaGaO_3$.

It was shown convincingly that two-phase composite electrodes comprising LSM and an oxygen-ion conducting solid-electrolyte phase reduce the polarization loss at the electrodes [10, 11]. Fluorite-structure electrolyte materials based on ZrO_2 and CeO_2 were added to the composites in the majority of studies dealing with composite cathodes of fuel cells. The optimal quantity of the electrolyte phase in composite electrodes is 40–50 mass % [12, 13], but may deviate from this value if sizes of crystallites in individual phases are largely different.

One more method, which facilitates the electrode reaction at the fuel cell cathodes, is the addition of various electrical catalysts into their structure [14–16]. The operating mechanism of the catalysts is determined by the increase in the speed of individual limiting stages and the expansion of the electrode reaction zone.

The main ideas about the mechanism of the oxygen reaction, which takes place on the electrodes made of mixed-conduction oxides, were formulated in experiments with LSM cathodes on ZrO_2 and/or CeO_2 electrolytes [17]. It follows from the general idea that the oxygen reaction on the cathode progresses by two parallel routes: 1) the stages of oxygen adsorption onto the surface of the mixed conductor followed by surface diffusion of oxygen particles to the three-phase boundary, ionization of oxygen, and incorporation of its ions into the electrolyte lattice near the three-phase boundary; 2) the stages of oxygen adsorption onto the surface of the mixed conductor followed by surface diffusion of oxygen atoms to the reaction site on the conductor surface, oxygen ionization, incorporation of oxygen ions into the lattice of the mixed conductor, diffusion of oxygen ions to the two-phase electrode–electrolyte boundary, and, finally, embedding of oxygen ions in the electrolyte lattice.

Thus, one of the factors determining the electrochemical activity of LSM and other oxide electrodes is the level of their oxygen non-stoichiometry. Defects on the electrode surface can act as reaction centers and influence the rate of adsorption–dissociation and surface diffusion processes [18]. Oxygen-ion conductivity of LSM is low (about 10^{-7} S cm^{-1} at 900° C [19]) and, therefore, the second route of the oxygen reaction is realized less often. Its role becomes significant only at a considerable cathodic polarization of LSM electrodes, leading to the increase in their electrochemical activity [20].

The behavior of LSM electrodes in combination with electrolytes based on lanthanum gallate, La(Sr)Ga(Mg)O_{3-x} (LSGM), is poorly studied and the available literature data indicate low electrochemical activity [21–27]. The reasons for this behavior are not quite clear; they may stem from both a slow rate of the electrochemical reaction in these electrode systems and the formation of a phase, which blocks the oxygen reaction, at the boundary between LSM and LSGM.

Most literature data do not explicitly suggest a considerable interaction of LSM and LSGM. For example, it was shown [21] that no changes occurred in X-ray diffraction patterns of fine, uniformly mixed sintered powders of LSM and LSGM even after 10 h sintering at 1,470° C, although some mutual diffusion of cations between LSM and LSGM was observed. Impurity phases were also not detected in LSM–LSGM composites sintered at 1,200° C for 2 h [28]. Judging by the results of an X-ray diffraction analysis [29], new phases were not formed when such mixed conductors as $La_{0.75}Sr_{0.2}Mn_{0.8}Co_{0.2}O_3$, $La_{0.8}Sr_{0.2}Mn_{0.8}Co_{0.2}O_3$, $Pr_{0.8}Sr_{0.2}Mn_{0.7}Co_{0.3}O_3$ and $Pr_{0.8}Sr_{0.2}Mn_{0.8}Co_{0.2}O_3$ were sintered with the solid electrolyte $La_{0.90}Sr_{0.10}Ga_{0.80}Mg_{0.20}O_{2.85}$ at 1,300° C for 300 h, although some migration of manganese into LSGM and gallium into the mixed conductors took place. When the LSM-LSGM composite was held at 650 and 1,000° C for 1,000 h, its components interacted very weakly; the manganese concentration in LSGM grains was about 2 mol%, while LSM grains were enriched a little in magnesium (about 1 mol%) and no gallium was detected [30, 31]. It was reported [32] that new compounds were not formed between LSM and LSGM up to 1,200° C, but the appearance of solid solutions was noted. The researchers [33] also stated the possibility of solid solutions being formed between LSM and LSGM at 1,300° C. They remarked, however, that an unambiguous conclusion about the mutual diffusion of cations between LSM and LSGM could not be drawn because the volume of the crystallographic unit cell changed insignificantly.

On the other hand, results of the studies [34–37] demonstrated that a single-phase region of solid solutions exists in the multi-component system La_2O_3–SrO–Ga_2O_3–MgO–Mn_2O_3 and manganese can be easily embedded in the structure of lanthanum gallate. A single-phase solid solution of the formula $La_{0.9}Sr_{0.1}(Ga_{0.9}Mn_{0.1})_{0.8}Mg_{0.2}O_{2.883-x+\delta}$ [35] and $La_{0.9}Sr_{0.1}Ga_{0.8}Mn_{0.2}O_{3-\delta}$ [36, 37] was synthesized. It was later shown that sintering of a mixture of powder oxides having the nominal composition $La_{0.9}Sr_{0.1}(Ga_{0.8}Mg_{0.1})_{1-x}Mn_xO_3$ at 1,500° C for 6 h led to the formation of a product with a cubic structure at $0 \le x \le 0.12$ [34].

Conductivity values of manganese-containing solid solutions based on lanthanum gallate also vary. For example, a relatively high conductivity of about 0.07 S/cm at 800° C was measured in $La_{0.9}Sr_{0.1}(Ga_{0.9}Mn_{0.1})_{0.8}Mg_{0.2}O_{2.883-x+\delta}$ [35], and 0.029÷0.046 S/cm in $La_{0.9}Sr_{0.1}Ga_{0.8}Mn_{0.2}O_{3-\delta}$ depending on the degree of manganese oxidation, also at 800° C [36, 37]. On the other hand, the studies [34] revealed that the conductivity dropped sharply as the LSM concentration increased to x=0.16 in $La_{0.9}Sr_{0.1}(Ga_{0.8}Mg_{0.1})_{1-x}Mn_xO_3$ and at x=0.16 the conductivity of the solid solution was 1–2 orders of magnitude lower than the conductivity of LSGM and 2.5–5 orders of magnitude lower than that of LSM.

The present study deals with a comparative analysis of the electrochemical behavior of different LSM electrodes in cells with LSGM and SDC electrolytes and determination of reasons for a low electrochemical activity of LSM electrodes in contact with the LSGM electrolyte.

Materials and methods

The solid electrolytes were synthesized using a two-stage solid-phase technology. La_2O_3, Ga_2O_3, $SrCO_3$ and $(MgCO_3)_4{\cdot}Mg(OH)_2{\cdot}5H_2O$ served as the initial materials for synthesis of the LSGM electrolyte of the formula $La_{0.88}Sr_{0.12}Ga_{0.82}Mg_{0.18}O_{2.85}$. Required amounts of the initial powders were mixed and ground in an agate mortar with isopropyl alcohol. The mixture was dried and calcined at 1,200° C for 2 h. The calcined mixture was ground again and samples were compacted under isostatic conditions at a pressure of 625 MPa. The compacts were sintered at 1,420° C for 10 h. The method for synthesis of the doped lanthanum gallate electrolyte is described in detail in [38].

Initial CeO_2 and Sm_2O_3 were mechanically activated in crushing cylinders of a planetary mill before synthesis of the SDC electrolyte. The pre-synthesis temperature of the SDC powders was 1,050° C. The SDC samples were sintered finally at 1,550° C for 3 h.

According to results of the X-ray diffraction analysis, the synthesized electrolytes were single-phase. The density of the electrolyte samples, which was measured by the Archimedes method in deionized water, accounted for 96–97% of the crystallographic density. Pellets about 1 mm thick and about 10 mm in diameter were cut out of the synthesized cylindrical electrolyte samples. The surface of the pellets was polished.

The electrodes were made using $La_{0.8}Sr_{0.2}MnO_3$, $La_{0.7}Sr_{0.3}MnO_3$, $Ce_{0.80}Sm_{0.20}O_{1.90}$, $La_{0.88}Sr_{0.12}Ga_{0.82}Mg_{0.18}O_{2.85}$ and $Zr_{0.82}Sc_{0.18}O_{1.91}$ powders, which were prepared by a standard ceramic technology. The pastes of composite electrodes were made by simultaneous grinding of $La_{0.8}Sr_{0.2}MnO_3$ with one of the electrolytes $Ce_{0.80}Sm_{0.20}O_{1.90}$ (SDC), $La_{0.88}Sr_{0.12}Ga_{0.82}Mg_{0.18}O_{2.85}$ (LSGM), or $Zr_{0.82}Sc_{0.18}O_{1.91}$ (SSZ) in the mass ratio 1:1. Fine suspensions of the electrode pastes with a butyral resin binder were brushed on both planes of the electrolyte pellets. The electrodes were about 50 μm thick. A current collector in the form of a $La_{0.6}Sr_{0.4}MnO_3$ layer about 150 μm thick was fired onto the external surface of the $La_{0.8}Sr_{0.2}MnO_3$+$Zr_{0.82}Sc_{0.18}O_{1.91}$ composite electrodes. Additional current collector was not added to any of the other electrodes. The sintering temperature of the electrodes was 1,150° C, with the exception of electrodes with additional current collector, which were fired at 1,200° C. The sintering time of all the electrodes was 2 h. Compositions of the electrode systems and the corresponding abbreviations are given in Table 1.

Platinum grids (0.1 mm wire, 0.5 mm pitch) served as current collectors to the electrodes. All the experiments were performed in air at temperatures of 500–850° C. The measuring cell temperature was adjusted and maintained to within ±1 degree by a TP-403 heat controller (VARTA).

Micrographs of the electrodes under study were taken using a JSM-5900LV scanning electron microscope. The phase composition of the electrode coatings was determined by the XDA method on a DMAX-2200 X-ray diffractometer (Rigaku). The electrochemical measurements were made by the method of impedance spectroscopy using an IM6 electrochemical set (Zahner Elektrik) at frequencies of 1 Hz to 100 kHz with an ac voltage amplitude of 10 mV. Recording of each impedance spectrum was followed by measurement of the total dc resistance of the electrochemical cell. The electrochemical cell was connected to the impedance meter in a two-electrode four-wire mode, providing elimination of the current leads' impedance from the total impedance of the system. The electrode polarization conductivity was calculated from the formula

$$\sigma_\eta = 2\left[S\left(R_{dc} - R_{hf}\right)\right]^{-1}, \quad (1)$$

where S is the electrode surface area, R_{dc} is the dc resistance of the electrochemical cell, and R_{hf} is the resistance, which is determined by extrapolation of the high-frequency branch of the impedance hodograph to the abscissa axis and corresponds to the ohmic resistance of the cell. The R_{hf} value generally includes the cell electrolyte resistance, the contact resistance, and some quantity of the electrode in-plane resistance. Each electrode system was studied both in the "pure" form as well as after modification by impregnation with a $Pr(NO_3)_3$ solution and subsequent thermal decomposition. This operation led to the distribution of fine praseodymium oxide, which is a

Table 1 Compositions of the electrode systems under study and the corresponding abbreviations

Abbreviations	Composition of the electrodes	Composition of the supporting electrolytes
LSM/LSGM	$La_{0.8}Sr_{0.2}MnO_3$	$La_{0.88}Sr_{0.12}Ga_{0.82}Mg_{0.18}O_{2.85}$
LSM1/LSGM	$La_{0.7}Sr_{0.3}MnO_3$	$La_{0.88}Sr_{0.12}Ga_{0.82}Mg_{0.18}O_{2.85}$
LSM–SDC/LSGM	50 mass % $La_{0.8}Sr_{0.2}MnO_3$+50 mass % $Ce_{0.80}Sm_{0.20}O_{1.90}$	$La_{0.88}Sr_{0.12}Ga_{0.82}Mg_{0.18}O_{2.85}$
LSM–SSZ/LSGM	50 mass % $La_{0.8}Sr_{0.2}MnO_3$+50 mass % $Zr_{0.90}Sc_{0.10}O_{1.95}$ (current collector — $La_{0.6}Sr_{0.4}MnO_3$)	$La_{0.88}Sr_{0.12}Ga_{0.82}Mg_{0.18}O_{2.85}$
LSM–LSGM/LSGM	50 mass % $La_{0.8}Sr_{0.2}MnO_3$+50 mass % $La_{0.88}Sr_{0.12}Ga_{0.82}Mg_{0.18}O_{2.85}$	$La_{0.88}Sr_{0.12}Ga_{0.82}Mg_{0.18}O_{2.85}$
LSM/SDC	$La_{0.8}Sr_{0.2}MnO_3$	$Ce_{0.80}Sm_{0.20}O_{1.90}$
LSM–SDC/SDC	50 mass % $La_{0.8}Sr_{0.2}MnO_3$+50 mass % $Ce_{0.80}Sm_{0.20}O_{1.90}$	$Ce_{0.80}Sm_{0.20}O_{1.90}$
LSM–SSZ/SDC	50 mass % $La_{0.8}Sr_{0.2}MnO_3$+50 mass % $Zr_{0.90}Sc_{0.10}O_{1.95}$ (current collector — $La_{0.6}Sr_{0.4}MnO_3$)	$Ce_{0.80}Sm_{0.20}O_{1.90}$
LSM–LSGM/SDC	50 mass % $La_{0.8}Sr_{0.2}MnO_3$+50 mass % $La_{0.88}Sr_{0.12}Ga_{0.82}Mg_{0.18}O_{2.85}$	$Ce_{0.80}Sm_{0.20}O_{1.90}$

highly active electrical catalyst of the oxygen reaction, in the porous matrix of the electrodes.

Results and discussion

It is seen from the micrographs of the electrodes under study (Fig. 1) that all the electrodes had very similar porosity and microstructure. Most particles in the electrodes were about 1 μm in size and some particles had the size of about 5 μm.

Figure 2 presents the temperature dependences of the electrode polarization conductivity of the test electrodes formed on LSGM and SDC electrolytes. For better visualization, the data for each of the electrodes formed on the SDC electrolyte are shown as filled dots/symbols and solid lines obtained by curve-fitting the data by the first- or second-order equations, while the data for the electrodes on the LSGM electrolyte are given as open dots/symbols not interconnected with lines. It is seen that the electrode polarization conductivity and, hence, the electrochemical activity of all the LSM-containing electrodes formed on the LSGM electrolyte were much smaller than those on the SDC electrolyte. An exception was the LSM–LSGM electrode on the SDC electrolyte, whose electrode conductivity proved to be as low as the electrode conductivity of the LSM electrodes on the LSGM electrolyte. For comparison, values of the electrode polarization conductivity of the LSM/LSGM electrode system, which were determined by other researchers [21, 25, 27], are also given in Fig. 2 as a separate dot [21] and dashed lines [25, 27]. They agree with our data.

Obviously, the reasons for high polarizability of the electrode system O_2, LSM/LSGM may be due either to the kinetic impediment to the electrode process or to the interaction between the contacting phases, which appears on the LSM/LSGM interface during the formation of the electrodes. In the latter case, the interaction product should have a high electric resistance and/or a low rate of oxygen exchange.

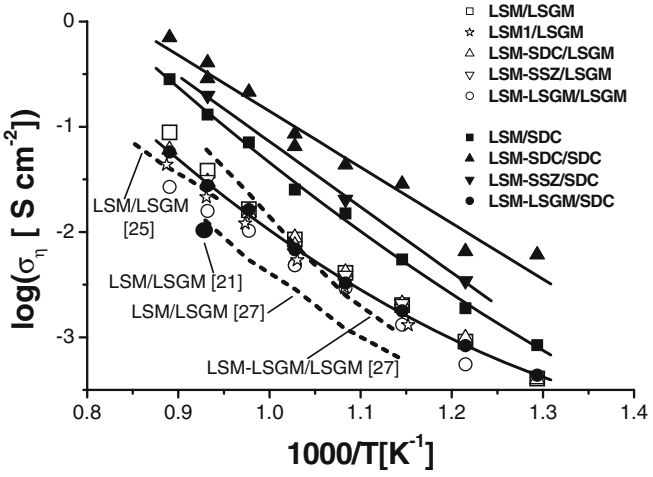

Fig. 2 Temperature dependence of the electrode polarization conductivity of the electrode systems under study

In this respect, an important result was that the electrode polarization conductivity of the LSM–LSGM electrode on the SDC electrolyte proved to be as low as the conductivity on the LSGM electrolyte. This behavior unambiguously suggests that a product of the interaction between lanthanum–strontium manganite and the lanthanum-gallate-based electrolyte is formed at the electrode sintering temperature (1,150° C). This explains the adverse role of the LSGM/LSM contact both when the LSM electrode is formed on the LSGM electrolyte and when LSGM is added to the LSM-based composite electrode as a ceramic component, while the supporting electrolyte was doped CeO_2, which does not interact with LSM and LSGM at 1,150° C.

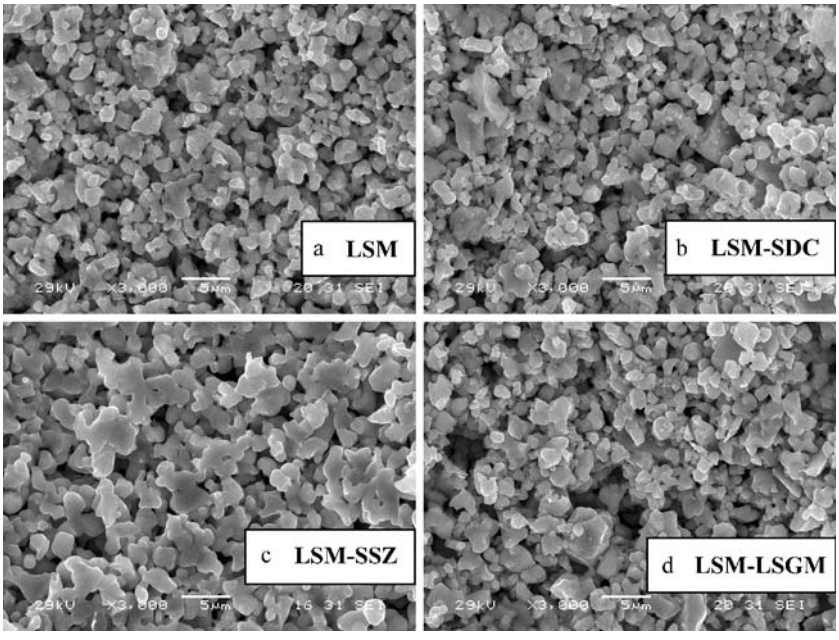

Fig. 1 Scanning electron microscopic images of the electrodes under study: **a** $La_{0.8}Sr_{0.2}MnO_3$ (LSM); **b** 50 mass % $La_{0.8}Sr_{0.2}MnO_3$+50 mass % $Ce_{0.80}Sm_{0.20}O_{1.90}$ (LSM-SDC); **c** 50 mass % $La_{0.8}Sr_{0.2}MnO_3$+50 mass % $Zr_{0.90}Sc_{0.10}O_{1.95}$ (LSM-SSZ); **d** 50 mass % $La_{0.8}Sr_{0.2}MnO_3$+50 mass % $La_{0.88}Sr_{0.12}Ga_{0.82}Mg_{0.18}O_{2.85}$ (LSM–LSGM)

Subsequent experiments were performed using the same electrode systems with the electrical catalyst PrO_{2-x} added to the electrodes. Figures 3 and 4 present histograms showing polarization conductivity values obtained at 800° C for the electrode systems under study before and after addition of PrO_{2-x}, respectively. It should be noted that the logarithmic scale of the polarization conductivity is used in Fig. 4, unlike in Fig. 3. As one would expect, the addition of the electrical catalyst to the electrodes caused considerable growth in the electrode polarization conductivity of all the electrode systems. However, while the electrochemical activity of the electrodes formed on the LSGM electrolyte increased 6–20 times, the corresponding parameter of the electrodes on the SDC electrolyte increased by a factor of 220–720. As the mechanism of the electrocatalytic action of PrO_{2-x} is connected with the expansion of the electrode reaction zone from the three-phase boundary to the surface of the electrolyte, which contacts the gaseous phase, this result presents a vivid demonstration that not only the LSM particles of the electrodes, but also the LSGM electrolyte itself changed when electrodes were formed on the LSGM electrolyte. If the region of the free surface of the LSGM electrolyte near LSM particles preserved its initial properties, the effect of the electrical catalyst would be much greater, similar to one observed in the LSM–LSGM/SDC electrode system.

Additional information about the behavior of the LSM and LSM-containing electrodes was obtained from the analysis of the ohmic resistance of the electrochemical cells under study. Figures 5 and 6 present the temperature dependences of the conductivity (σ_{el}) of LSGM and SDC electrolytes, respectively, which were determined from the high-frequency branch of the impedance spectra and geometrical dimensions of the cells using the formula

$$\sigma_{el} = L/(R_{hf}S), \tag{2}$$

where L is the thickness of the electrolyte pellet and S is the electrode surface area. The thick solid line in both figures denotes the temperature dependences of the actual conductivity of the corresponding electrolytes, which were determined in special experiments.

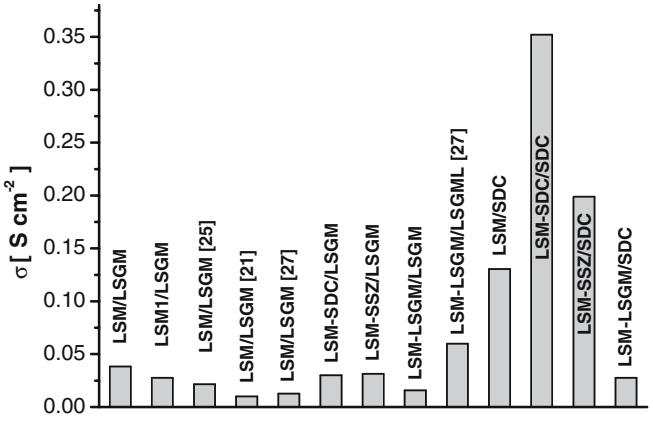

Fig. 3 Electrode polarization conductivity of the electrode systems under study at 800° C

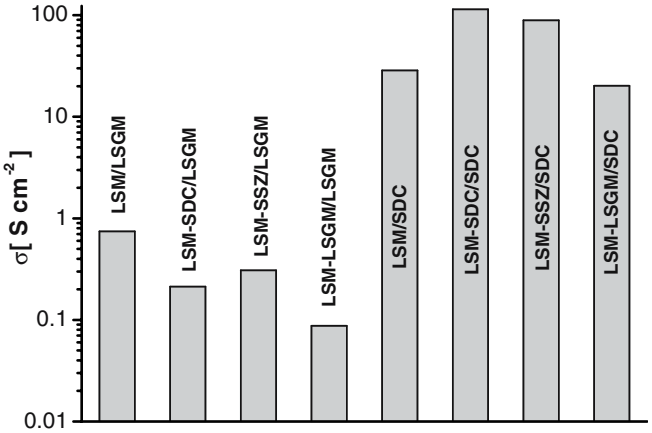

Fig. 4 Electrode polarization conductivity of the electrode systems under study at 800° C after addition of the electrical catalyst PrO_2 to the porous matrix of the electrodes

It is seen from Fig. 5 that the ohmic resistance of the cells with the supporting LSGM electrolyte, except the cell with the double-layer LSM–SSZ electrode whose external $La_{0.6}Sr_{0.4}MnO_3$ layer served as the current collector, was much higher than that expected from considerations of the electrolyte conductivity. The ohmic resistance of the cell is especially high in the case of composite LSM–LSGM electrodes. The dashed lines in the same figure show analogous data, which were obtained [26] from measurements of the ohmic resistance of LSM/LSGM half-cells (the sintering temperatures of electrodes are shown in Fig. 5 near the corresponding literature data). It is seen that they agree fairly well with our data.

It is known that the ohmic resistance of solid-electrolyte cells may be higher than the resistance calculated from the electrolyte conductivity due to a variety of reasons. Such causes as considerable peeling of the electrode from the electrolyte and an insulation layer of large thickness between the electrode and the electrolyte will not be

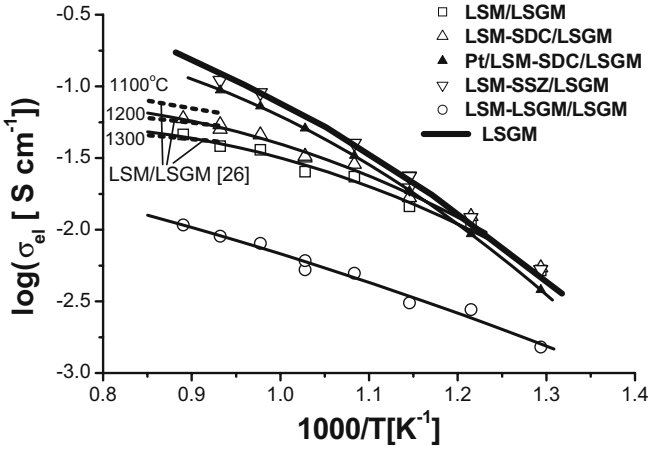

Fig. 5 Conductivity of the LSGM electrolyte, which was determined from the ohmic resistance of the cells with the LSGM electrolyte

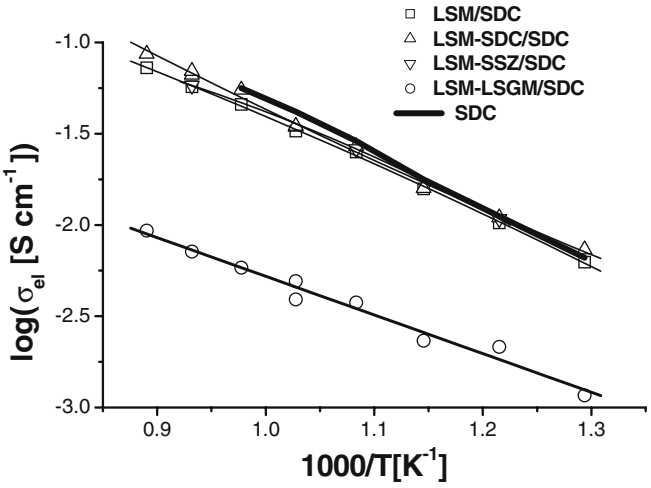

Fig. 6 Conductivity of the SDC electrolyte, which was determined from the ohmic resistance of the cells with the SDC electrolyte

discussed in this paper, since they certainly bear no relevance to the systems under study. In our case, one of the more realistic reasons may be the so-called "contact" resistance, which is due to the porous structure of the electrodes and, correspondingly, incomplete covering of the electrolyte surface with the electrode material (the current constriction effect) [39]. A further explanation is that a non-uniform current is distributed over the electrode volume when the current collector, e.g., a metal grid, contacts the external surface of the electrode in some points only, while the electron conduction of the electrode material is insufficient so as to ensure a uniform flow of the current in the electrode [40].

It was already noted that in the case of the double-layer LSM–SSZ electrodes with the $La_{0.6}Sr_{0.4}MnO_3$ current collector, the conductivity, which was calculated from the ohmic resistance and the geometry of the cell, coincided with the conductivity of the LSGM electrolyte over the whole temperature interval studied (Fig. 5). To probe the importance of the current collector, the experiment with the LSM–SDC/LSGM sample was repeated after covering the surface of the LSM–SDC electrode with the thin layer of fine platinum. It is seen from Fig. 5 that, in that case, the conductivity of electrolyte determined from the ohmic resistance of the cell became very close to the actual electrolyte conductivity.

It can, therefore, be concluded that a well-organized current collector ensures a uniform distribution of the current over the electrolyte. This indicates that the reason for the high ohmic resistance of the cells with the gallate electrolyte is an insufficient in-plane conductivity of the electrodes rather than the contact resistance on the electrode–electrolyte interface (the current constriction effect). This conclusion is supported by the fact that the experimentally determined conductivity of the electrolyte differs from the true conductivity, the larger the higher the temperature. This is because the activation energy of the electrolyte conductivity is much larger than the activation energy of the electrode material conductivity. The experimental findings and theoretical calculations [41] suggest the same character of deviations caused by a non-uniform distribution of the current density over the electrolyte owing to the finite resistance of the electrode material.

Thus, the in-plane electrode conductivity considerably decreased in the cells with the gallate electrolyte due to its interaction with LSM. On the contrary, it is seen from Fig. 6 that the conductivity, which was determined from the ohmic resistance of the cells with the supporting SDC electrolyte, approaches the conductivity of this electrolyte in each case. Thus, no serious problems with the distribution of the current in the cells with the cerium electrolyte were encountered. The only exception was the result obtained for the cell with the LSM–LSGM electrodes, in which the determined conductivity was as low as that observed in the cells with the LSGM-supporting electrolyte. If we use the data of Figs. 5 and 6 and calculate to what extent the experimental value of the electrolyte resistivity differs from the true value, the difference will

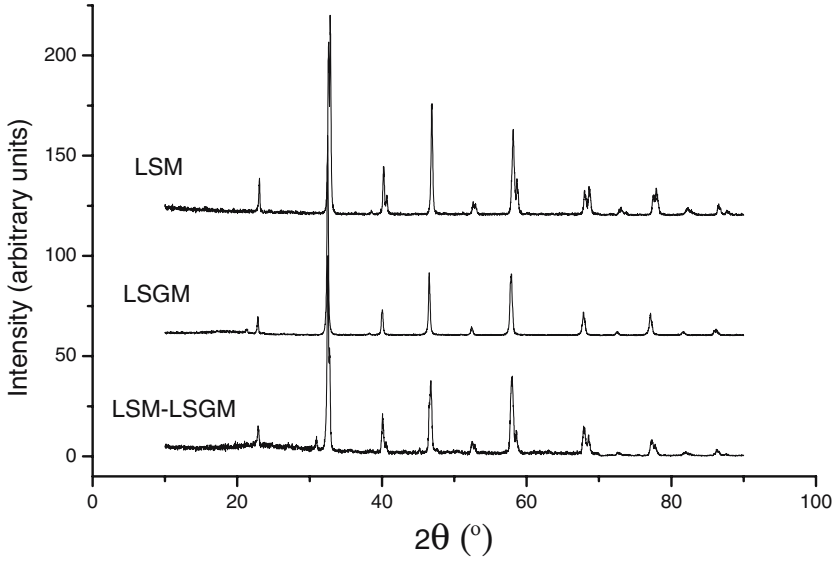

Fig. 7 X-ray diffraction patterns of the LSM–LSGM composite, which was heat-treated under conditions of the electrode sintering (1150° C, 2 h), and those of the initial components of this composite

depend little on the electrolyte in the case of LSM–LSGM composite electrodes. For example, for the cells with the LSGM and SDC electrolytes, the difference is 442 and 670 Ohm cm at 500° C and is yet closer at 800° C, namely, 101 and 122 Ohm cm, respectively. Clearly, these resistivity values are determined mainly by insulation properties of the LSM–LSGM electrodes, which appear during the interaction of the LSM and LSGM phases in the electrodes.

Thus, the electrochemical experiments provide unique proof that the interaction between LSM and LSGM causes the formation of a product with low conductivity. However, we were unable to detect the interaction product by direct methods: neither the X-ray diffraction analysis nor the micro-probe X-ray analysis yielded conclusive evidence.

Results of the X-ray diffraction analysis are given in Fig. 7. The X-ray diffraction pattern of the composite comprising $La_{0.8}Sr_{0.2}MnO_3$ and $La_{0.88}Sr_{0.12}Ga_{0.82}Mg_{0.18}O_{2.85}$, which was sintered under the conditions used for sintering of the electrodes to the electrolyte, is a superposition of the spectra of the initial components of the composite. The only distinction is the new line at 2θ=30.9°, which is located near the base lines of such compounds as $LaSrGa_3O_7$ and $LaSrGaO_4$. A similar result was obtained in [30, 31], but traces of these compounds are often present in highly doped lanthanum gallate and have little influence on the conductivity of the main phase.

The interaction product could not be detected, probably because the reaction layer on the LSM/LSGM interface was thin, the compounds had a similar elementary composition, and the peaks were spaced close to one another in the X-ray diffraction patterns of these phases.

Indeed, from the literature data, it follows that the micro-probe X-ray analysis reveals the mutual diffusion of cations between LSM and LSGM only at temperatures higher than the temperature of the electrode formation used in our experiments (1,150° C). For example, the micro-probe analysis of LSM electrodes, which were sintered onto the LSGM electrolyte at 1,200 and 1,300° C for 2 h, showed that the reaction layer was 6 and 9 μm thick, respectively [26, 42]. Sintering of LSM and LSGM at 1,300° C for 1 h leads to manganese diffusion to a distance of 2–4 μm [43]. It was reported [29] that manganese diffused to LSGM up to 20–30 μm and a small quantity of gallium passed from LSGM to the neighboring phase when such mixed conductors as $La_{0.75}Sr_{0.2}Mn_{0.8}Co_{0.2}O_3$, $La_{0.8}Sr_{0.2}Mn_{0.8}Co_{0.2}O_3$, $Pr_{0.8}Sr_{0.2}Mn_{0.7}Co_{0.3}O_3$ and $Pr_{0.8}Sr_{0.2}Mn_{0.8}Co_{0.2}O_3$ were sintered with the solid electrolyte $La_{0.90}Sr_{0.10}Ga_{0.80}Mg_{0.20}O_{2.85}$ at 1,300° C for 300 h. It was shown [21] that at 1,470° C the region of the mutual diffusion between LSM and LSGM was about 20 μm. La, Sr, and Mg were redistributed between the phases, while a considerable mutual diffusion of Mn to LSGM and Ga to LSM was not observed.

The question why solid solutions, which are formed during the interaction of LSM and LSGM, have such low conductivity has not been studied, but promises to be interesting. For example, the researchers [34] supposed that manganese has an adverse effect on the conductivity of lanthanum gallate because the concentration of vacancies, which is a maximum in the initial highly doped lanthanum gallate, decreases upon additional dissolution of an amount of manganese. However, special studies need to be conducted to verify this hypothesis.

In closing, it is necessary to add that, despite the interaction discovered between LSM and LSGM (detected and proven due to the fact that the interaction product is highly resistive), to make a final conclusion on the origin of the low electrochemical activity of the LSM electrodes in contact with LSGM electrolyte is untimely. Either insulation properties of the formed interaction product or its low electrocatalytic activity due to the low oxygen exchange could be a reason for its low electrode polarization conductivity.

Conclusions

The comparative analysis of the electrochemical behavior of LSM electrodes and composite electrodes comprising a mixture of LSM and LSGM or LSM and SDC, and also LSM and SSZ in cells with supporting electrolytes LSGM and SDC, showed that in the electrode systems where LSM and LSGM contact each other, the formation of the electrodes is accompanied by the interaction between LSM and LSGM, leading to the appearance of an insulating product that blocks the oxygen reaction.

Acknowledgements The authors wish to thank the Russian Foundation for Basic Research for the financial support of Project No. 04-03-96084, under which this study was performed. They are grateful to Z. Martemyanova for her XRD assistance, to A. Pankratov for his help in obtaining SEM images, and especially to Alex Pickering for her assistance in critically reading the manuscript.

References

1. Ishihara T, Matsuda H, Takita Y (1994) J Am Chem Soc 116:3801
2. Feng M, Goodenough JB (1994) Eur J Solid State Inorg Chem 31:663
3. Matsui T, Inaba M, Mineshige A, Ogumi Z (2005) Solid State Ion 176:647
4. Akikusa J, Adachi K, Hoshino K, Ishihara T, Takita Y (2001) J Elecrochem Soc 148:A1275
5. Kuroda K, Hashimoto I, Adachi K, Akikusa J, Tamou Y, Komada N, Ishihara T, Takita Y (2000) Solid State Ion 132:199
6. Wang S, Kato T, Nagata S, Kaneko T, Iwashita N, Honda T, Dokiya M (2002) Solid State Ion 152–153:477
7. Milliken C, Guruswamy S (2002) J Am Ceram Soc 85:2479
8. Kamata H, Yonemura Y, Mizusaki J, Tagawa H, Naraya K, Sasamoto T (1995) J Phys Chem Solids 56:943
9. Poirson A, Decorse P, Caboche G, Dulfour LC (1997) Solid State Ion 99:287
10. Kenjo T, Osawa S, Fujikawa K (1991) J Electrochem Soc 138:349
11. Tanner CW, Fung KZ, Virkar AV (1997) J Electrochem Soc 144:21
12. Murray EP, Barnett A (2001) Solid State Ion 143:265
13. Kim JD, Kim GD, Moon JW, Park Y, Lee WH, Kobayashi K, Nagai M, Kim CE (2001) Solid State Ion 143:379

14. Yamahara K, Jacobson CP, Visco SJ, Zhang XF, De Jonghe LC (2005) Solid State Ion 176:275
15. Yamahara K, Jacobson CP, Visco SJ, De Jonghe LC (2005) Solid State Ion 176:451
16. Sahibzada M, Benson SJ, Rudkin RA, Kilner JA (1998) Solid State Ion 113–115:285
17. Adler SB (2004) Chem Rev 104:4791
18. Yasumoto K, Mori N, Mizusaki J, Tagawa H, Dokiya M (2001) J Electrochem Soc 148:A105
19. Yasuda I, Ogasawara K, Hishinuma M, Kawada T, Dokiya M (1996) Solid State Ion 86–88:1197
20. Lee HY, Cho WS, Oh SM, Wiemhöfer HD, Göpel W (1995) J Electrochem Soc 142:2659
21. Huang K, Feng M, Goodenough JB, Schmerling M (1996) J Electrochem Soc 143:3630
22. Huang K, Feng M, Goodenough JB, Milliken C (1997) J Electrochem Soc 144:3620
23. Huang K, Goodenough J (2000) J Alloys Compd 303–304:454
24. Huang K, Wan J, Goodenough JB (2001) J Mater Sci 36:1093
25. Wang S, Lu X, Liu M (2002) J Solid State Electrochem 6:384
26. Yi JY, Choi GM (2004) J Eur Ceram Soc 24:1359
27. Gong W, Goplan S, Pal UB (2005) J Electrochem Soc 152: A1890
28. Armstrong TJ, Virkar AV (2002) J Electrochem Soc 149:A1565
29. Naoumidis A, Ahmad-Khanlou A, Samardzija Z, Kolar D (1999) Fresenius Z Anal Chem 365:277
30. Rozumek M, Majewski P, Mandlener T, Aldinger F (2002) Mat-wiss Werkstofftech 33:348
31. Rozumek M (2003) Kristallchemische Eigenschaften ausgewählter Funktions-Kermiken im quasi-quaternären System Ga_2O_3–La_2O_3–MgO–SrO. Thesis, Stuttgart
32. Wang W, Hellstrom EE (1996) Mat Res Soc Symp Proc 411:261
33. Pelosato R, Sora IN, Dotelli G, Ruffo R, Mari CM (2005) J Eur Ceram Soc 25:2587
34. Yi JY, Choi GM (2002) Solid State Ion 148:557
35. Trofimenko N, Ullmann H (1999) Solid State Ion 118:215
36. Thangadurai V, Shukla AK, Gopalakrishnan J (1998) Chem Commun, p2647
37. Sebastian L, Shukla AK, Gopalakrishnan J (2000) Bull Mater Sci 23:169
38. Gorelov VP, Bronin DI, Sokolova JV, Näfe H, Aldinger F (2001) J Eur Ceram Soc 21:2311
39. Fleig J, Pham P, Sztulzaft P, Maier J (1998) Solid State Ion 113–115:739
40. Jiang SP, Love JG, Apateanu L (2003) Solid State Ion 160:15
41. Perfiliev MV, Demin AK, Kuzin BL, Lipilin AS (1988) High-temperature Electrolysis of Gases. Moscow, Nauka (in Russian)
42. Yi JY, Choi GM (2004) Solid State Ion 175:145
43. Pelosato R, Sora IN, Ferrari V, Dotelli G, Mari CM (2004) Solid State Ion 175:87